Research on Engineering Structures & Materials
www.jresm.org
MIM Research Group

Research Article

Short-span bending–shear and modified axial-loading response of locally sourced laminated petung bamboo: A preliminary study

Bastian Artanto Ampangallo [*,a], Memed Timang Palembangan [b]

Dept. of Civil Engineering, Faculty of Engineering, Universitas Kristen Indonesia Toraja, Indonesia

Article Info

Article History:

Received 26 Jun 2026

Accepted 12 Sep 2026

Keywords:

Laminated petung bamboo;
Dendrocalamus asper;
Short-span bending-shear;
Modified axial loading;
Nominal flexural stress;
Nominal axial stress;
Bio-composite material

Abstract

This study presents a preliminary evaluation of locally sourced laminated petung bamboo (Dendrocalamus asper) fabricated using PVAC Crossbond X4 adhesive and tested under short-span bending–shear and modified axial-loading configurations. Petung bamboo from North Toraja, Indonesia, was processed into longitudinal strips and bonded into rectangular laminated members. The fabrication records indicated a moisture content of 12.0 ± 1.5% and a density of 720 ± 45 kg/m^3. Three specimens were tested under short-span four-point bending–shear, and three specimens were tested under modified axial loading. The bending specimens had dimensions of 600 mm × 20 mm × 150 mm, with a support span of 450 mm and a shear span of 150 mm, resulting in L/h = 3 and a/h = 1. Therefore, the bending response may include shear deformation, local bearing, local indentation, inter-laminar stress transfer, and deep-beam-type behavior. The modified axial-loading specimens had a height of approximately 600 mm and a loaded cross-section of 20 mm × 150 mm, without independent lateral restraint. Under short-span bending–shear loading, the maximum loads were 13.13, 11.73, and 9.00 kN, with an average nominal flexural stress of 11.28 MPa. Under modified axial loading, the maximum axial loads ranged from 361.69 to 374.02 kN, with an average nominal axial stress of 123.08 MPa. Visual observations indicated fiber cracking or buckling, local crushing, lateral deformation, and apparent inter-laminar separation. The results provide preliminary comparative evidence for laminated petung bamboo, but they should not be interpreted as standardized material-strength properties or design-level values.

© 2026 MIM Research Group. All rights reserved.

1. Introduction

The construction sector is increasingly encouraged to explore renewable, bio-based, and locally available materials to support more sustainable material development [1,2]. This trend is consistent with broader developments in bio-based composite systems, where renewable polymers and natural-resource-based materials are increasingly explored for sustainable material applications [3]. Among various bio-based resources, bamboo has attracted considerable attention because of its rapid growth, low self-weight, favorable strength-to-weight ratio, and relatively short harvesting cycle compared with conventional timber [1,2]. In Indonesia, petung bamboo (Dendrocalamus asper) is one of the promising bamboo species for engineered material development because of its large culm diameter, thick culm wall, and favorable physical and mechanical characteristics [2,4,5].

However, the direct use of natural bamboo culms in structural components is limited by their hollow circular cross-section, tapered geometry, nodes, irregular dimensions, and natural variability in density and fiber distribution [2,6]. These characteristics make it difficult to obtain

*Corresponding author: bastian@ukitoraja.ac.id
[a]orcid.org/0009-0004-4354-235X; [b]orcid.org/0009-0008-0429-4313
DOI: http://dx.doi.org/10.17515/resm2026-1794me0626rs

standardized members with predictable mechanical response [6,7]. Laminated bamboo offers a practical alternative by converting bamboo culms into strips and bonding them into engineered members with more uniform geometry, improved dimensional stability, and more controlled member configuration [6–9].

The mechanical response of laminated bamboo is governed not only by the intrinsic strength of bamboo fibers, but also by lamina arrangement, fiber orientation, adhesive bonding, surface preparation, pressing condition, moisture condition, density, and manufacturing quality [8,9]. Bonding performance is particularly important because adhesive type, surface condition, pressure, and interfacial quality can influence stress transfer and failure behavior in bamboo-based composite materials [10,11]. Previous studies on laminated bamboo members also show that product configuration, specimen geometry, and loading arrangement can affect bending response and structural performance [12,13]. Studies on laminated fibre-reinforced composites further indicate that reinforcement content, matrix condition, and laminate architecture can influence thermo-mechanical performance and damage development [14]. In layered bio-composite members, reinforcement distribution, interfacial interaction, morphology, and local defects can significantly affect mechanical response and damage development [15]. Therefore, experimental evaluation is required to clarify the load-carrying response, nominal stress, displacement behavior, and visually observed failure characteristics of laminated bamboo members produced using specific local materials and fabrication procedures [8–13].

Although engineered bamboo has been widely investigated, experimental data on locally sourced laminated petung bamboo from Indonesia remain limited, particularly for Dendrocalamus asper strips bonded with PVAC-based adhesive [4,5,11]. This gap is important because bamboo source, adhesive type, lamination process, specimen geometry, loading arrangement, span-to-depth ratio, end-contact condition, and lateral restraint condition can substantially influence the measured mechanical response [8–13]. Therefore, results obtained from a specific local bamboo source and a specific laboratory test configuration should be interpreted within the limitations of the adopted specimen geometry, fabrication procedure, and loading arrangement [8–13].

The novelty of this study lies in providing preliminary experimental information on locally sourced laminated Dendrocalamus asper fabricated using PVAC Crossbond X4 adhesive and tested under short-span bending–shear and modified axial-loading configurations. The main contribution of this study is not to establish generalized design values or standardized material-strength properties, but to provide initial evidence on the load-carrying response, nominal flexural stress, nominal axial stress, displacement behavior, and visually observed damage characteristics of locally produced laminated petung bamboo. In lightweight composite applications, optimization of laminate composition, reinforcement proportion, and manufacturing quality is important to achieve reliable thermo-mechanical performance [16]. Therefore, this study aims to evaluate the short-span bending–shear response and modified axial-loading response of locally sourced laminated petung bamboo as a preliminary step toward the development of renewable bio-composite members for lightweight and non-primary structural applications.

2. Materials and Methods

2.1 Materials

The material used in this study was petung bamboo (Dendrocalamus asper) obtained from Lembang To'yasa Akung, Bangkelekila' District, North Toraja, Indonesia. The selected bamboo culms were estimated to be approximately three to four years old based on local source information and field selection during material preparation. This age range was selected because mature bamboo generally has a more developed fiber structure, thicker culm wall, and more suitable characteristics for engineered bamboo member production. Petung bamboo was selected due to its relatively large culm diameter and favorable physical characteristics for laminated bamboo fabrication [2,4,5]. The laminated specimens were manufactured from longitudinal bamboo strips bonded using PVAC Crossbond X4 adhesive.

Table 1. Material and specimen characteristics

Category	Parameter	Description / Value
Material source	Bamboo species	Petung bamboo (Dendrocalamus asper)
Material source	Source location	Lembang To'yasa Akung, Bangkelekila' District, North Toraja, Indonesia
Material source	Bamboo age	3-4 years
Material source	Number of bamboo culms	3 culms
Material source	Number of bamboo clumps	1–2 clumps from the same local sampling area
Material source	Culm-height location	Not specifically recorded in the laboratory fabrication record
Material source	Radial strip position	Not specifically recorded in the laboratory fabrication record
Material source	Node/strip selection	Internode-dominant strips; nodes were avoided or minimized where possible, particularly in the critical test regions
Material source	Specimen independence	Specimens were prepared from laminated blocks produced using strips from the same local bamboo source; independent manufacturing of each specimen was not fully documented
Fabrication	Adhesive	PVAC Crossbond X4
Fabrication	Adhesive specification	Commercial PVAC-based adhesive; detailed technical data such as solids content, viscosity, recommended service environment, and manufacturer datasheet values were not available in the laboratory record
Fabrication	Adhesive spread rate	250 g/m^2
Fabrication	Surface preparation	Both bonding surfaces were planed before adhesive application
Fabrication	Number of bamboo strips	45 strips
Fabrication	Average strip thickness	3.3 mm
Fabrication	Bamboo strip arrangement	Longitudinal arrangement
Fabrication	Fiber orientation	Parallel to the primary loading direction
Fabrication	Drying method	Natural air-drying; strips were placed approximately 30 cm above the ground
Fabrication	Drying duration	14 days
Fabrication	Moisture content	12.0 ± 1.5%
Fabrication	Density	720 ± 45 kg/m^3
Fabrication	Pressing method	Cold pressing after adhesive application and longitudinal strip arrangement
Fabrication	Pressing pressure	0.8 MPa
Fabrication	Pressing duration	24 h
Fabrication	Conditioning time	7 days at room temperature before cutting and testing
Fabrication	Final bond line thickness	0.10–0.20 mm
Specimen geometry	Nominal short-span bending–shear specimen dimension	600 mm × 20 mm × 150 mm
Specimen geometry	Nominal modified axial-loading specimen dimension	600 mm specimen height with 20 mm × 150 mm loaded cross-section
Specimen geometry	S1 PBL, short-span bending–shear	Length = 600 mm; width = 20 mm; depth = 150 mm
Specimen geometry	S2 PBL, short-span bending–shear	Length = 600 mm; width = 20 mm; depth = 150 mm
Specimen geometry	S3 PBL, short-span bending–shear	Length = 600 mm; width = 20 mm; depth = 150 mm

Specimen geometry	S1, modified axial loading	Height = 600 mm; width = 20 mm; depth = 150 mm; loaded area = 3,000 mm^2
Specimen geometry	S2, modified axial loading	Height = 600 mm; width = 20 mm; depth = 150 mm; loaded area = 3,000 mm^2
Specimen geometry	S3, modified axial loading	Height = 600 mm; width = 20 mm; depth = 150 mm; loaded area = 3,000 mm^2
Testing	Testing location	Structure and Materials Laboratory, Hasanuddin University, Gowa, Indonesia

Note: Parameters described as "not specifically recorded" were not available in the laboratory fabrication record. The specimen dimensions shown in this table are the nominal dimensions retained in the laboratory record and used for stress calculations. Individual measured dimensions should be reported in future studies to improve dimensional traceability and reduce uncertainty in nominal stress calculation.

The longitudinal arrangement was adopted to align the bamboo fibers with the primary loading direction and to produce rectangular laminated members with more uniform geometry than natural bamboo culms. The specimens were prepared for two loading configurations, namely short-span bending–shear and modified axial loading.

The material characterization and fabrication records included bamboo source, estimated bamboo age, strip arrangement, adhesive type, moisture content, density, adhesive spread rate, pressing pressure, pressing duration, conditioning time, strip thickness, bond line thickness, and specimen dimensions. These parameters were measured, recorded, or applied during specimen preparation. However, they were not systematically varied or statistically evaluated as independent variables in this preliminary study. Therefore, their individual effects on bonding quality, nominal stress, displacement response, and damage characteristics could not be quantified.

2.2 Preparation of Laminated Petung Bamboo Specimens

The preparation of laminated petung bamboo specimens began with the selection of mature bamboo culms and their conversion into longitudinal strips according to the required specimen dimensions. Internode-dominant strips were prioritized, and nodes were avoided or minimized where possible, particularly in the critical test regions. The bamboo strips were naturally air-dried for 14 days by placing them approximately 30 cm above the ground to reduce direct contact with soil moisture and to allow air circulation during drying.



Fig. 1. Laminated petung bamboo specimen prepared for mechanical testing

After drying, both bonding surfaces of the bamboo strips were planned to obtain smoother surfaces and more uniform lamina thickness. The prepared strips were then coated with PVAC Crossbond X4 adhesive at an applied spread rate of approximately 250 g/m^2 and arranged longitudinally so that the bamboo fibers were aligned with the primary loading direction. The adhesive-coated strips

were assembled into rectangular laminated blocks and cold-pressed at approximately 0.8 MPa for 24 h.

After pressing, the laminated blocks were conditioned at room temperature for 7 days before final cutting and testing. The final specimens were finished using a planer and saw to obtain the required rectangular dimensions for short-span bending–shear and modified axial-loading tests. This preparation process was intended to reduce the natural irregularity of bamboo culms and to produce laminated members with more uniform geometry for mechanical testing. Nevertheless, because laminated bamboo behaves as a layered bio-composite material, its mechanical response may still be affected by strip quality, fiber alignment, surface preparation, adhesive distribution, pressing quality, moisture condition, density, and inter-laminar bonding condition. Figure 1 shows the laminated petung bamboo specimen prepared for the experimental program.

2.3 Short-Span Bending–Shear Test Procedure

Static short-span four-point bending–shear testing was conducted to evaluate the load-carrying response, nominal flexural stress, midspan displacement response, and failure characteristics of the laminated petung bamboo specimens. Three specimens, coded S1 PBL, S2 PBL, and S3 PBL, were tested using a Universal Testing Machine equipped with a data logger and an externally mounted displacement transducer. The test was performed using a four-point loading configuration with two symmetrical loading points. Because the support span was relatively short compared with the specimen depth, the test was interpreted as a short-span combined bending–shear test rather than a conventional standardized flexural-strength test.

Table 2. Short-span bending–shear test configuration of laminated petung bamboo specimens

Parameter	Value
Loading configuration	Four-point loading with two symmetrical loading points
Test interpretation	Short-span combined bending–shear response
Specimen length	600 mm
Support span, (L)	450 mm
Overhang on each side	75 mm
Distance from support to nearest loading point, (a)	150 mm
Specimen width, (b)	20 mm
Specimen depth, (h)	150 mm
Support-span-to-depth ratio, (L/h)	3.0
Shear-span-to-depth ratio, (a/h)	1.0
Number of specimens	3
Specimen codes	S1 PBL, S2 PBL, S3 PBL
Load definition	(P) = total load recorded by the testing machine; each loading point = (P/2)
Displacement measurement	Midspan displacement measured using an externally mounted displacement transducer

The total specimen length was 600 mm, while the effective support span, (L), was 450 mm, leaving an overhang of 75 mm at each end. The distance from each support to the nearest loading point, (a), was 150 mm. The specimen width, (b), and depth, (h), were 20 mm and 150 mm, respectively. Therefore, the support-span-to-depth ratio was L/h = 3, and the shear-span-to-depth ratio was a/h = 1. These ratios indicate that the test configuration may involve not only bending effects but also shear deformation, local bearing, local indentation near the loading points, inter-laminar shear, and deep-beam-type behavior.

During testing, each specimen was positioned horizontally on two lower cylindrical supports and loaded vertically through two upper loading rollers. The load recorded by the testing machine was defined as the total applied load, (P). Accordingly, each loading point transferred one-half of the total load, (P/2), to the specimen. This definition was used consistently in the bending-moment and

nominal stress calculations to avoid a factor-of-two error in load interpretation. The load was applied monotonically until each specimen reached its maximum load and visible failure condition. Load and midspan displacement data were recorded throughout the test to describe the response of each specimen under the adopted short-span bending–shear configuration.

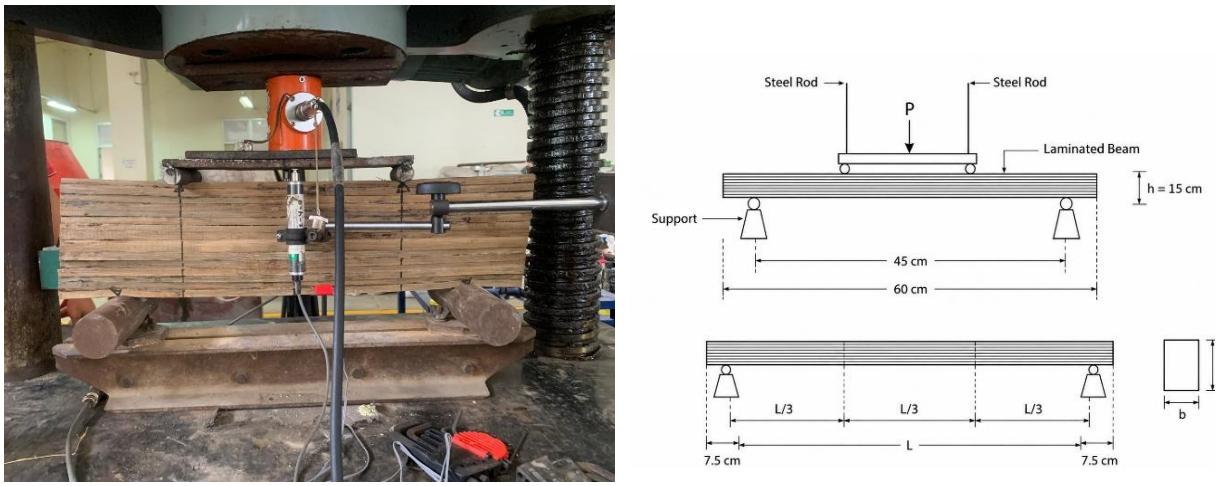


Fig. 2. Short-span four-point bending–shear test configuration: (a) experimental setup and (b) schematic showing the total applied load (P), two equal point loads (P/2), support span (L = 450) mm, shear span (a = 150) mm, specimen width (b = 20) mm, and specimen depth (h = 150) mm

The nominal flexural stress was calculated based on the adopted four-point loading configuration. The general bending stress equation is expressed as:

$$\sigma f = My/I \tag{1}$$

where σf is the nominal flexural stress, (M) is the maximum bending moment, (y) is the distance from the neutral axis to the outermost fiber, and (I) is the second moment of area of the rectangular cross-section.

For a rectangular cross-section, the nominal flexural stress can be expressed as:

$$\sigma f = 6Mmax/(bh^2) \tag{2}$$

where σf is the nominal flexural stress, Mmax is the maximum bending moment, b is the specimen width, and h is the specimen depth.

In the adopted four-point loading configuration, the total applied load recorded by the testing machine was defined as (P). This total load was transferred to the specimen through two equal loading points; therefore, each loading point applied (P/2). The maximum bending moment in the constant-moment region can be expressed as:

$$Mmax = \frac{Pa}{2} \tag{3}$$

where (P) is the total maximum load recorded by the testing machine and (a) is the distance from the support to the nearest loading point.

Therefore, the nominal flexural stress can be calculated as:

$$\sigma f = 3Pa/(bh^2) \tag{4}$$

where (P) is the total maximum load recorded by the testing machine, (a) is the distance from the support to the nearest loading point, (b) is the specimen width, and (h) is the specimen depth.

It should be emphasized that the calculated value represents nominal flexural stress under the adopted short-span combined bending–shear configuration. Because the support-span-to-depth

ratio and shear-span-to-depth ratio were relatively low, namely L/h = 3 and a/h = 1, the result should not be interpreted as a standardized material flexural-strength value.

Figure 2 shows the flexural test configuration of laminated petung bamboo specimens: (a) experimental setup and (b) schematic of four-point bending with two symmetrical loading points.

2.4 Modified Axial Loading Test Procedure

Static modified axial loading was conducted to evaluate the member-level axial resistance, nominal axial stress, axial displacement response, and failure characteristics of the laminated petung bamboo specimens. Three specimens, coded S1, S2, and S3, were tested using a Universal Testing Machine under axial loading parallel to the longitudinal fiber direction of the laminated bamboo strips. The loaded cross-sectional area of each specimen was determined from the measured width and depth, while the specimen height was approximately 600 mm.

Because of the relatively large specimen height compared with the weak-axis dimension, the axial-loading configuration may be influenced by specimen slenderness, initial straightness, end-contact condition, platen alignment, load eccentricity, local instability, or column-type behavior. Therefore, the test results were interpreted as member-level axial resistance and nominal axial stress under the adopted modified axial-loading configuration, not as standardized compression-parallel-to-fiber material strength.

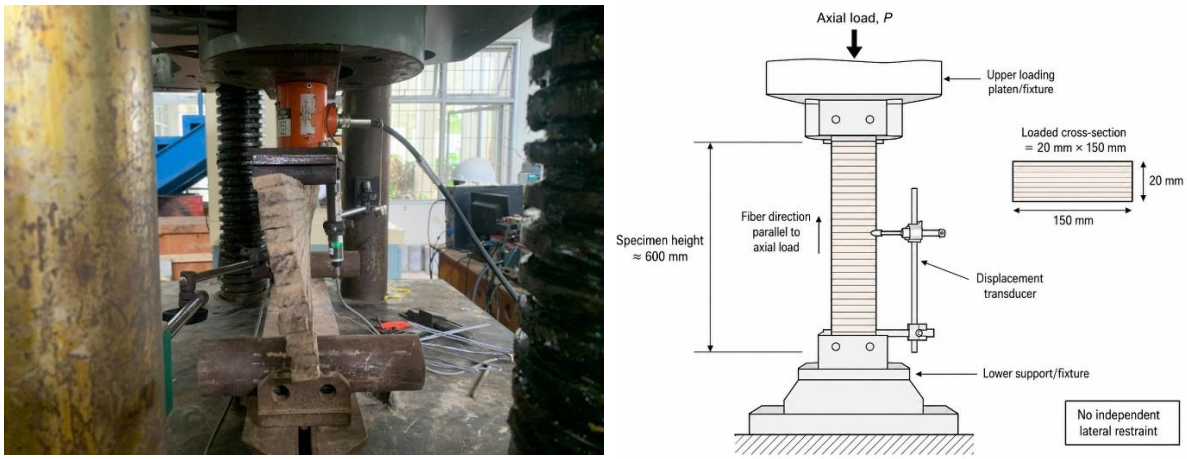


Fig. 3. Modified axial-loading configuration of laminated petung bamboo specimens: (a) experimental setup during testing and (b) schematic representation showing the axial loading direction, specimen height of approximately 600 mm, loaded cross-section of 20 mm × 150 mm, fiber direction parallel to the axial load, displacement transducer position, and loading/support conditions

Before testing, the dimensions of each specimen were measured to determine the loaded cross-sectional area used in the nominal axial stress calculation. Each specimen was placed vertically between the upper and lower steel compression platens of the Universal Testing Machine. The specimen ends were positioned in contact with the platens, and the specimen was manually centered and aligned with the loading axis to minimize eccentric loading. No independent lateral restraint was applied along the specimen height during testing. Therefore, possible slenderness-related effects and alignment sensitivity were considered when interpreting the axial response. The axial load was applied monotonically until each specimen reached its maximum load and visible failure condition. The applied load and axial displacement were recorded using the testing-machine data-acquisition system. The recorded displacement was used to describe the axial response of the laminated petung bamboo specimens, including the initial load increase, peak-load stage, and post-peak tendency where available. Since the displacement was obtained from the testing system, it may include specimen deformation, platen seating, fixture movement, local indentation, and machine compliance. Therefore, the displacement values were interpreted as axial crosshead displacement rather than direct material strain.

The nominal axial stress was calculated using:

$$\sigma a = Pmax/A \quad (5)$$

where σa is the nominal axial stress, Pmax is the maximum axial load recorded by the testing machine, and (A) is the loaded cross-sectional area of the specimen. Because the test was conducted using a modified laboratory-based axial-loading configuration, the calculated nominal axial stress should be interpreted within the limitations of the adopted specimen geometry, loading alignment, end-contact condition, specimen slenderness, and test setup.

Figure 3 shows the modified axial-loading setup used for the laminated petung bamboo specimens.

2.5 Testing Machine and Data Acquisition

The mechanical tests were conducted at the Structure and Materials Laboratory, Department of Civil Engineering, Faculty of Engineering, Hasanuddin University, Gowa, Indonesia. Both the short-span bending–shear test and the modified axial-loading test were performed using a hydraulic universal testing machine of Tinius Olsen type. The available photographic documentation indicated a load-cell capacity of 50 tf, equivalent to approximately 490 kN. For the short-span bending–shear test, the specimen was supported by two lower cylindrical steel supports and loaded through two upper steel loading rollers attached to a steel spreader/loading plate. The support span was set to 450 mm, while the distance from each support to the nearest loading point was 150 mm. The lower support diameter and upper loading roller diameter were approximately 75 mm and 25 mm. These approximate values were not used in the stress calculation. The load was recorded by the testing-machine data logger, while the midspan displacement was measured using an external LVDT/displacement transducer positioned at the specimen midspan.

For the modified axial-loading test, the specimen was placed vertically between the upper steel loading platen/fixture and the lower steel support/fixture. The specimen was manually centered on the lower fixture and aligned with the vertical loading axis of the testing machine before loading. No independent lateral restraint was applied along the specimen height. Therefore, the effective unsupported length was considered to be approximately equal to the specimen height of 600 mm. Initial straightness and load eccentricity were not measured quantitatively; however, initial straightness was visually checked, and eccentricity was minimized through manual centering and alignment. During testing, load and displacement data were recorded using the integrated testing-machine data logger connected to the load cell and external displacement transducer. For the short-span bending–shear test, the reported displacement represents the midspan displacement measured by the external displacement transducer. For the modified axial-loading test, the reported axial displacement should be interpreted as the displacement response under the adopted test setup and may include specimen deformation, platen contact, fixture movement, local indentation, and machine compliance. The available testing-machine and data-acquisition parameters are summarized in Table 5.

Table 3. Testing machine and data-acquisition parameters

Parameter	Short-span bending–shear test	Modified axial-loading test
Testing location	Structure and Materials Laboratory, Department of Civil Engineering, Faculty of Engineering, Hasanuddin University, Gowa, Indonesia	Structure and Materials Laboratory, Department of Civil Engineering, Faculty of Engineering, Hasanuddin University, Gowa, Indonesia
Testing machine	Hydraulic universal testing machine, Tinius Olsen type	Hydraulic universal testing machine, Tinius Olsen type
Load-cell capacity	50 tf, equivalent to approximately 490 kN	50 tf, equivalent to approximately 490 kN
Calibration status	Calibration certificate number and calibration date were not available in the laboratory test record	Calibration certificate number and calibration date were not available in the laboratory test record
Control mode	Monotonic vertical loading using the UTM	Monotonic axial loading using the UTM
Loading rate	2.0 mm/min	1.0 mm/min

Data-acquisition system	*Integrated testing-machine data logger connected to the load cell and external displacement transducer*	Integrated testing-machine data logger connected to the load cell and external displacement transducer
Data-acquisition frequency	1 Hz	1 Hz
Loading fixture	Two upper steel loading rollers mounted below a steel spreader/loading plate	Upper steel loading platen/fixture used to transfer axial load
Support fixture	Two lower cylindrical steel supports mounted on the UTM base fixture	Lower steel support/fixture used to provide bearing support during axial loading
Support span	450 mm, measured as the distance between the two lower cylindrical supports	Full bearing contact between the lower end of the specimen and the steel support fixture; no bending support span was used
Shear span/loading distance	150 mm, measured as the distance between each support and the nearest loading point	Load applied concentrically along the specimen axis; no separate shear span or loading distance was used
Lower support diameter	Approximately 75 mm	Lower support was a flat steel bearing fixture/platen rather than cylindrical rollers
Upper loading roller diameter	Approximately 25 mm	Upper loading was applied through a flat steel platen/fixture rather than rollers
Platen/fixture dimensions	Upper loading was applied through a steel spreader plate carrying two rollers; approximate plate width 50-75 mm and thickness 10-15 mm	Approximate steel platen/fixture size 200 mm x 200 mm with steel bearing plate thickness about 10-20 mm
Seating preload	Approximately 0.5 kN	Approximately 1.0 kN
Displacement measurement	Midspan displacement measured using an external LVDT/displacement transducer positioned at the specimen midspan	Axial displacement measured using an external LVDT/displacement transducer aligned with the loading direction
Alignment procedure	Specimen was centered on the two lower cylindrical supports, and the two upper loading rollers were aligned with the marked loading points before testing	Specimen was manually centered on the lower fixture and aligned with the vertical loading axis of the UTM before testing
Specimen end/contact condition	Contact occurred between the specimen and the upper loading rollers/lower supports at the designated loading and support points	Specimen ends were placed in direct contact with the upper and lower steel loading fixtures
Effective unsupported length	N/A	Approximately equal to the specimen height, 600 mm, because no independent lateral restraint was applied along the specimen height
Initial straightness measurement	N/A	Not measured quantitatively; initial straightness was visually checked before testing
Load eccentricity measurement	N/A	Not measured quantitatively; eccentricity was minimized through manual centering and alignment
Lateral restraint	N/A	No independent lateral restraint was applied along the specimen height
Instability observation	N/A	Possible lateral deformation or local instability was visually observed during axial loading and considered in interpreting the axial response

2.6 Data Analysis

The experimental data were analyzed to evaluate the preliminary short-span bending–shear response and modified axial-loading response of laminated petung bamboo specimens. The analysis focused on the load-carrying response, nominal stress values, displacement behavior, and visually observed failure characteristics. Because this study used a limited number of specimens and adopted non-standardized testing configurations, the calculated stress values were interpreted as nominal responses under the specific experimental conditions rather than standardized material-strength properties or design values.

For the short-span bending–shear test, the main parameters analyzed were maximum load, maximum bending moment, nominal flexural stress, load–midspan displacement response, displacement at peak load, and visually observed failure mode. The maximum bending moment was calculated based on the adopted four-point loading configuration, in which the total load recorded by the testing machine was defined as (P), and each loading point transferred (P/2) to the specimen. The nominal flexural stress was calculated using the rectangular-section bending equation described in Section 2.3. However, because the support-span-to-depth ratio was L/h = 3 and the shear-span-to-depth ratio was a/h = 1, the calculated nominal flexural stress was not interpreted as a standard flexural-strength value. Instead, it was used to compare the tested specimens under the same short-span combined bending–shear configuration.

For the modified axial-loading test, the main parameters analyzed were maximum axial load, nominal axial stress, axial displacement response, displacement at peak load, and visually observed failure characteristics. The nominal axial stress was calculated by dividing the maximum axial load by the loaded cross-sectional area of each specimen. Because the specimens had a relatively large height compared with the weak-axis dimension and no independent lateral restraint was applied along the specimen height, the axial results were interpreted as member-level axial resistance under the adopted modified axial-loading configuration. Therefore, the reported nominal axial stress should not be interpreted as standardized compression-parallel-to-fiber material strength.

The displacement data were interpreted according to the measurement configuration used in each test. For the short-span bending–shear test, the displacement response refers to the midspan displacement measured using an external LVDT/displacement transducer. For the modified axial-loading test, the axial displacement response may include specimen deformation, platen contact, fixture movement, local indentation, and machine compliance. Therefore, the recorded axial displacement was used only to describe the response trend under the adopted test setup and was not converted into material strain or modulus values.

Descriptive statistics were used to summarize the experimental results. The mean value, standard deviation, and coefficient of variation were calculated for each main response parameter. Since only three specimens were tested for each loading configuration, the statistical evaluation was limited to descriptive comparison among the tested specimens and was not intended for inferential analysis or population-level generalization.

Failure characteristics were evaluated through visual observation after testing. The observed damage patterns were used to support the interpretation of the load–displacement response. However, because no microscopic observation, bond line shear test, delamination test, or bamboo-failure-percentage analysis was conducted, the proposed failure mechanisms were treated as possible interpretations rather than experimentally confirmed causes.

3. Results and Discussion

3.1 Short-Span Bending–Shear Load Capacity and Nominal Flexural Stress

The short-span bending–shear response of laminated petung bamboo was evaluated based on the maximum load recorded during the adopted four-point loading configuration. In this test, the load recorded by the testing machine was defined as the total applied load, (P), and each loading point transferred (P/2) to the specimen. The test was interpreted as a short-span combined bending–shear test because the support-span-to-depth ratio was L/h = 3, while the shear-span-to-depth

ratio was a/h = 1. Therefore, the calculated values are reported as nominal flexural stress under the adopted short-span bending–shear configuration and should not be interpreted as standardized flexural-strength values.

As summarized in Table 6, the maximum loads recorded for S1 PBL, S2 PBL, and S3 PBL were 13.13 kN, 11.73 kN, and 9.00 kN, respectively. The corresponding nominal flexural stresses were 13.13 MPa, 11.73 MPa, and 9.00 MPa. The average maximum load and average nominal flexural stress were both 11.28, expressed in kN and MPa, respectively. Among the tested specimens, S1 PBL showed the highest short-span bending–shear response, followed by S2 PBL and S3 PBL.

The coefficient of variation of the nominal flexural stress was 18.62%, indicating moderate variation among the three tested specimens. This variation may be associated with bamboo strip quality, lamina arrangement, fiber alignment, adhesive distribution, bonding condition, and local defects. Since only three specimens were tested, this variation should be interpreted descriptively and should not be generalized as population-level material variability. Overall, the results provide preliminary comparative information on the nominal response of locally produced laminated petung bamboo under the adopted short-span bending–shear configuration.

Table 4. Short-span bending–shear test results of laminated petung bamboo specimens

Specimen	Maximum load, Pmax (kN)	Maximum load, Pmax (N)	Nominal flexural stress, σf (MPa)	Interpretation
S1 PBL	13.13	13,128.10	13.13	Highest response among the tested specimens
S2 PBL	11.73	11,728.60	11.73	Intermediate response
S3 PBL	9.00	8,996.40	9.00	Lowest response among the tested specimens
Average	11.28	11,284.37	11.28	Descriptive mean of three specimens
Standard deviation	2.10	2,101.37	2.10	Descriptive variation among the tested specimens
Coefficient of variation (%)	18.62	18.62	18.62	Variation among the three tested specimens only

Note: The reported stress values represent nominal flexural stress under the adopted short-span bending–shear configuration with L/h = 3 and a/h = 1. These values should not be interpreted as standardized flexural-strength values or design-level material properties.

Figure 4 illustrates the maximum load recorded for each laminated petung bamboo specimen under the adopted short-span bending–shear configuration.

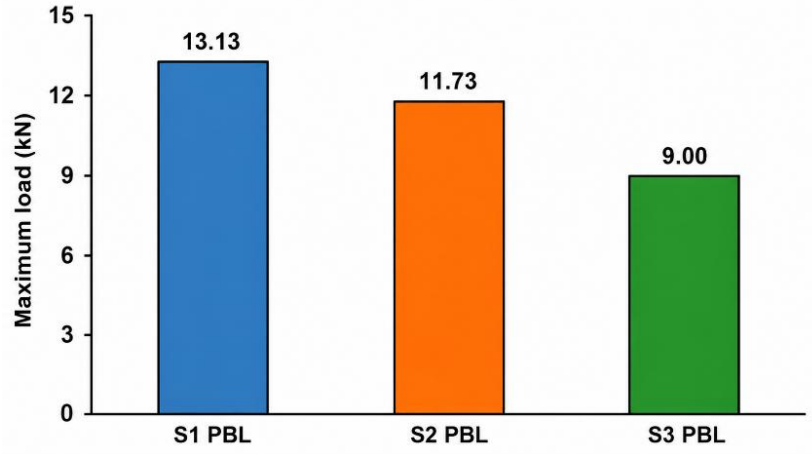


Fig. 4. Maximum load of laminated petung bamboo specimens under the adopted short-span bending–shear configuration

3.2 Load–Midspan Displacement Response under Short-Span Bending–Shear Loading

The load–midspan displacement response of the laminated petung bamboo specimens is presented in Figure 5. The displacement was measured at the midspan region using an external displacement transducer. In general, the curves showed an initial approximately linear response, followed by nonlinear behavior as the load approached the maximum value. This response indicates that the laminated section was initially able to transfer load effectively, while progressive stiffness degradation occurred as local damage developed during loading.

The curves should be interpreted within the limitations of the adopted short-span bending–shear configuration. Because the support-span-to-depth ratio was L/h = 3 and the shear-span-to-depth ratio was a/h = 1, the measured response may include bending deformation, shear deformation, local bearing, local indentation near the loading and support points, and inter-laminar stress transfer. Therefore, the curves should not be interpreted as conventional flexural load–deflection behavior or used to derive standard flexural material properties.

Among the tested specimens, S1 PBL reached the highest load, followed by S2 PBL and S3 PBL. This order is consistent with the maximum load results presented in Table 6 and Figure 4. The differences in load–midspan displacement response may be associated with bamboo strip quality, lamina arrangement, fiber alignment, adhesive distribution, bonding condition, and local defects. The nonlinear part of the curves suggests the possible development of tensile fiber cracking, compression damage near the loading region, shear-related deformation, inter-laminar slip, or local delamination. However, these mechanisms are treated only as possible interpretations because no microscopic observation, bond line shear test, or controlled delamination assessment was conducted. Overall, the load–midspan displacement curves provide comparative response indicators for the tested specimens under the adopted short-span bending–shear configuration. They should not be used to establish modulus of elasticity, standardized flexural strength, or design-level stiffness parameters.

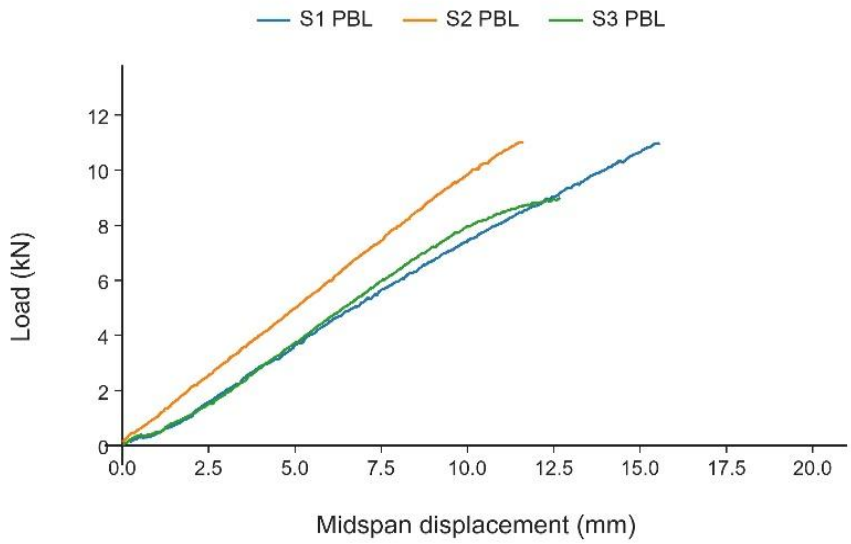


Fig. 5. Load–midspan displacement curves of laminated petung bamboo specimens under the adopted short-span bending–shear configuration

3.3 Modified Axial-Loading Response and Nominal Axial Stress

The modified axial-loading response of the laminated petung bamboo specimens was evaluated based on maximum axial load, recorded axial displacement, nominal axial stress, and visually observed deformation characteristics. As summarized in Table 7, the maximum axial loads recorded for S1, S2, and S3 were 361.69 kN, 374.02 kN, and 372.02 kN, respectively. The corresponding recorded axial displacements were 10.41 mm, 10.66 mm, and 8.51 mm. The average maximum axial load was 369.24 kN, while the average recorded axial displacement was 9.86 mm.

Based on the loaded cross-sectional area of 20 mm × 150 mm, the nominal axial stresses were 120.56 MPa, 124.67 MPa, and 124.01 MPa for S1, S2, and S3, respectively. The average nominal axial stress was 123.08 MPa, with a coefficient of variation of 1.79%. This coefficient of variation indicates limited variation among the three tested specimens only and should not be interpreted as evidence of general material consistency or population-level reliability.

Table 5. Modified axial-loading test results of laminated petung bamboo specimens

Specimen	Maximum axial load, Pmax (kN)	Recorded axial displacement (mm)	Nominal axial stress, σa (MPa)	Interpretation
S1	361.69	10.41	120.56	Member-level axial response
S2	374.02	10.66	124.67	Member-level axial response
S3	372.02	8.51	124.01	Member-level axial response
Average	369.24	9.86	123.08	Descriptive mean of three specimens
Standard deviation	6.62	1.18	2.21	Descriptive variation among the tested specimens
Coefficient of variation (%)	1.79	11.92	1.79	Limited variation among the three tested specimens only

Note: The reported stress values represent nominal axial stress under the adopted modified axial-loading configuration. They should not be interpreted as standardized compression-parallel-to-fiber material strength or design-level material properties.

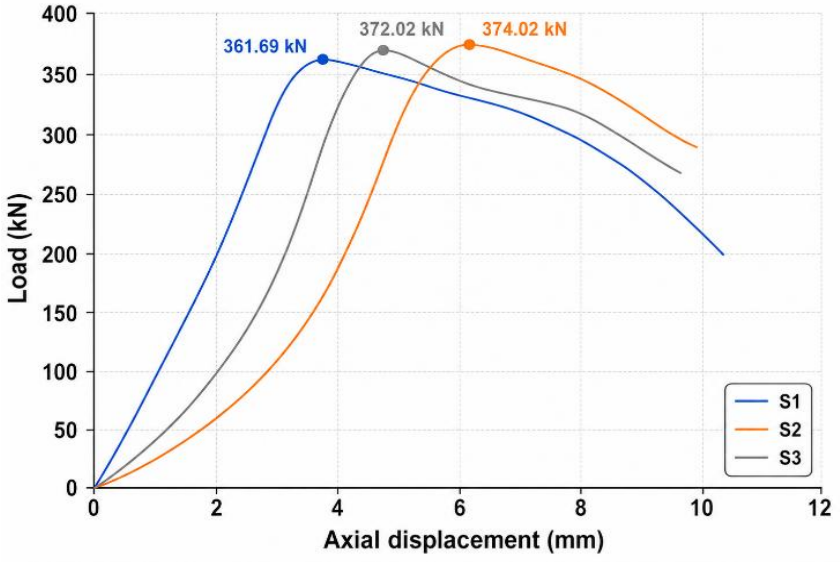


Fig. 6. Load–axial displacement curves of laminated petung bamboo specimens under the adopted modified axial-loading configuration

The axial results should be interpreted within the limitations of the adopted modified axial-loading configuration. The specimens had a height of approximately 600 mm and a loaded cross-section of 20 mm × 150 mm. Since no independent lateral restraint was applied along the specimen height, the response may have been influenced by specimen slenderness, end-contact condition, alignment, possible load eccentricity, platen contact, local crushing, and local instability. Therefore, the reported values represent member-level axial resistance and nominal axial stress under the

adopted modified axial-loading configuration, not standardized compression-parallel-to-fiber material strength.

Figure 6 presents the load–axial displacement curves of the laminated petung bamboo specimens. The curves show an initial increase in load followed by nonlinear displacement behavior as deformation and local damage developed. The recorded axial displacement may include specimen deformation, platen contact, fixture movement, local indentation, and machine compliance. Therefore, the curves are used only as comparative response indicators under the adopted modified axial-loading configuration and are not used to derive material strain, modulus, or design-level axial properties.

3.4 Failure Characteristics and Possible Damage Mechanisms

Failure characteristics were observed after the short-span bending–shear and modified axial-loading tests to identify the dominant visible damage patterns of the laminated petung bamboo specimens. These observations were used to support the interpretation of the load–displacement responses, but they were not intended to confirm detailed failure mechanisms at the material or bond line level.

Under the short-span bending–shear configuration, the observed damage was mainly associated with tensile-side fiber cracking, localized damage near the loading and support regions, and apparent separation between several laminated layers. These damage patterns indicate that the response of laminated petung bamboo was influenced by the interaction between bamboo fibers, lamina arrangement, adhesive bonding, and stress transfer between adjacent layers. However, because no microscopic observation, bond line shear test, delamination test, or bamboo-failure-percentage analysis was conducted, inter-laminar slip, adhesive-interface degradation, and delamination are discussed only as possible damage mechanisms rather than experimentally confirmed causes.



(a) (b) (c)

Fig. 7. Observed damage characteristics of laminated petung bamboo specimens after modified axial loading: (a) S1, (b) S2, and (c) S3, showing local crushing, fiber buckling, lateral deformation, and apparent inter-laminar separation

Under the modified axial-loading configuration, the specimens showed visible damage associated with axial loading parallel to the longitudinal fiber direction, as shown in Figure 7. The main observed damage patterns included local crushing, fiber buckling, lateral deformation, and apparent separation between laminated layers. These observations suggest that the axial response may have been influenced by fiber alignment, end-contact condition, bonding quality, specimen slenderness, and local instability. Therefore, the axial failure characteristics should be interpreted as member-level response under the adopted modified axial-loading configuration, not as standardized compression-parallel-to-fiber material failure.

Overall, the observations indicate that laminated petung bamboo behaves as a layered bio-composite member whose response depends on bamboo strip quality, fiber orientation, lamina arrangement, adhesive distribution, interfacial bonding, local defects, and manufacturing quality. This interpretation is consistent with the general behavior of composite materials, where mechanical properties are affected by reinforcement characteristics, interfacial interaction, morphology, and local defects [15]. Further investigation using microscopic observation, bond line shear testing, controlled delamination assessment, and larger specimen sets is required to confirm the detailed failure mechanisms of laminated petung bamboo.

3.5 Quantitative Comparison with Previous Studies

A quantitative comparison between the present study and selected engineered bamboo studies is presented in Table 8. Only studies with clearly reported numerical values were selected to reduce the use of unreported parameters. The comparison is intended to position the present results within the broader context of engineered bamboo research. However, direct equivalence should not be assumed because the reported values are affected by bamboo species, product type, adhesive system, pressing condition, specimen geometry, loading direction, testing standard, span-to-depth ratio, and sample size.

3.6 Structural Implications, Limitations, and Future Work

The results suggest that locally sourced laminated petung bamboo has potential for further development as a renewable bio-composite member for lightweight and non-primary structural applications. However, this implication should be interpreted cautiously because the reported values represent preliminary nominal responses obtained under the adopted short-span bending–shear and modified axial-loading configurations. Therefore, the results should not be used directly as standardized material properties or design-level parameters.

Several limitations should be acknowledged. First, only three specimens were tested for each loading configuration, so the results describe variation among the tested specimens rather than population-level material reliability. Second, the bending test used low span ratios, namely $L/h = 3$ and $a/h = 1$, which may have introduced shear deformation, local bearing, local indentation, inter-laminar stress transfer, and deep-beam-type behavior. Third, the axial test used a 600 mm-high specimen with a 20 mm × 150 mm loaded cross-section and no independent lateral restraint; therefore, the response may have been influenced by specimen slenderness, end-contact condition, alignment, possible load eccentricity, platen contact, and local instability.

Although several fabrication parameters were measured, recorded, or applied during specimen preparation, including moisture content, density, adhesive spread rate, pressing pressure, pressing duration, conditioning time, strip thickness, and bond line thickness, these variables were not systematically varied or statistically evaluated as independent factors. In addition, direct strain measurement, modulus evaluation, microscopic observation, bond line shear testing, controlled delamination assessment, durability testing, creep testing, connection testing, and full-scale component testing were not conducted. These limitations restrict the use of the present results to preliminary comparative interpretation.

Future studies should use larger sample sizes, standardized engineered-bamboo testing procedures, independently manufactured specimens, controlled fabrication variables, direct strain measurement, and detailed failure characterization. Durability, moisture sensitivity, creep behavior, connection performance, fire performance, and full-scale component behavior should also be evaluated before laminated petung bamboo is recommended for broader building applications. Fire-related assessment is particularly important because bio-composite and polymer-bonded composite materials require adequate flammability and fire-behavior evaluation before being used as building components [20].

Table 6. Quantitative comparison of the present study with selected engineered bamboo studies

Study	Material / product	Species	MC / density	Adhesive / processing condition	Test configuration
Rofii et al. [4]	Laminated bamboo board	Dendrocalamus asper	MC = 15.25%; density = 0.66 g/cm^3	PVAc adhesive; glue spread = 280 g/m^2; pressing pressure = 1 MPa	Static bending test; specimen size = 300 mm × 20 mm × 20 mm; BS 373 and ASTM D1037 basis
Li et al. [17]	Laminated bamboo lumber beam	Laminated bamboo lumber	—	Adhesive-bonded laminated bamboo lumber	Beam bending test; (n = 20) specimens
Al-Rukaibawi et al. [18]	Laminated bamboo lumber N-finity	Moso bamboo	MC = 7.2%; density = 625 kg/m^3	Commercial laminated bamboo lumber product	ISO 23478-2022 compression test; (n = 16) specimens per direction
Wang et al. [19]	Bamboo scrimber	Bamboo scrimber	—	Phenol formaldehyde resin; hot-pressed scrimber product	Compression tests in longitudinal, radial, and tangential directions
Present study	Locally sourced laminated petung bamboo	Dendrocalamus asper	MC = 12.0 ± 1.5%; density = 720 ± 45 kg/m^3	PVAC Crossbond X4; spread rate = 250 g/m^2; pressing pressure = 0.8 MPa; pressing duration = 24 h; conditioning = 7 days	Short-span bending–shear and modified axial loading; specimen size = 600 mm × 20 mm × 150 mm; (L/h = 3), (a/h = 1); (n = 3) for each configuration
Rofii et al. [4]	MOR = 100.55 MPa	—	MOE = 11.66 GPa	Same species, but different specimen geometry, product configuration, and bending test basis	
Li et al. [17]	MOR = 63.95 MPa	—	MOE = 10.91 GPa	Conventional beam-level bending response; not directly equivalent to the present short-span bending–shear test	
Al-Rukaibawi et al. [18]	—	Compression parallel-to-grain = 68 MPa	Compression modulus = 8.75 GPa	Standardized compression reference for LBL; different species, product, and axial test configuration	
Wang et al. [19]	—	Longitudinal compressive strength = 94.67 MPa	Longitudinal compression modulus = 14.61 GPa	Useful compression-failure reference, but the product type differs from laminated petung bamboo	
	Nominal flexural stress = 11.28 MPa	Nominal axial stress = 123.08 MPa	Not evaluated as MOE	Preliminary nominal response under the adopted test configurations; not a design-level material property	

Note: The dash symbol (—) indicates that the parameter was not the main reported result in the selected study. The values reported for the present study represent nominal responses under the adopted short-span bending–shear and modified axial-loading configurations. They should not be interpreted as standardized material-strength properties or design-level values.

4. Conclusions

This study presented a preliminary evaluation of locally sourced laminated petung bamboo (Dendrocalamus asper) fabricated using PVAC Crossbond X4 adhesive and tested under short-span

bending–shear and modified axial-loading configurations. Three specimens were tested for each loading configuration. The analysis focused on maximum load, nominal stress, displacement response, and visually observed damage characteristics. The results should be interpreted as preliminary nominal responses under the adopted laboratory configurations rather than standardized material-strength properties or design-level values.

Under short-span bending–shear loading, the specimens reached maximum loads of 13.13 kN, 11.73 kN, and 9.00 kN for S1 PBL, S2 PBL, and S3 PBL, respectively. The corresponding nominal flexural stresses were 13.13 MPa, 11.73 MPa, and 9.00 MPa, with an average value of 11.28 MPa and a coefficient of variation of 18.62%. Because the test used L/h = 3 and a/h = 1, these values represent nominal flexural stress under the adopted short-span bending–shear configuration and should not be interpreted as standardized flexural-strength values.

Under modified axial loading, the specimens reached maximum axial loads of 361.69 kN, 374.02 kN, and 372.02 kN for S1, S2, and S3, respectively. The corresponding nominal axial stresses were 120.56 MPa, 124.67 MPa, and 124.01 MPa, with an average value of 123.08 MPa. The coefficient of variation of 1.79% indicates limited variation among the three tested specimens only. Since the axial test used a 600 mm-high specimen with a 20 mm × 150 mm loaded cross-section and no independent lateral restraint, the results represent member-level axial resistance under the adopted modified axial-loading configuration, not standardized compression-parallel-to-fiber material strength.

Visual observations indicated local crushing, fiber cracking or buckling, lateral deformation, and apparent inter-laminar separation. These damage patterns suggest that the response of laminated petung bamboo was influenced by bamboo strip quality, fiber alignment, lamina arrangement, adhesive distribution, interfacial bonding, local defects, and manufacturing quality. However, because no microscopic observation, bond line shear test, controlled delamination assessment, or bamboo-failure-percentage analysis was conducted, the proposed damage mechanisms should be regarded as possible interpretations rather than experimentally confirmed causes.

Overall, the findings provide preliminary comparative evidence for the further development of locally sourced laminated petung bamboo for lightweight and non-primary structural applications. Broader application requires larger sample sizes, standardized testing procedures, controlled fabrication variables, direct strain measurement, durability assessment, creep testing, connection testing, fire-performance evaluation, and full-scale component testing before reliable design-level parameters can be established.

Acknowledgements

The authors acknowledge the support provided by the Department of Civil Engineering, Faculty of Engineering, Universitas Kristen Indonesia Toraja. The authors also express their appreciation to the Structure and Materials Laboratory of Hasanuddin University, Gowa, Indonesia, for providing the experimental testing facilities used in this study.

References

[1] Adier MFV, Sevilla MEP, Valerio DNR, Ongpeng JMC. Bamboo as sustainable building materials: A systematic review of properties, treatment methods, and standards. Buildings. 2023;13(10):2449. https://doi.org/10.3390/buildings13102449

[2] Chaowana K, Wisadsatorn S, Chaowana P. Bamboo as a sustainable building material-culm characteristics and properties. Sustainability. 2021;13(13):7376. https://doi.org/10.3390/su13137376

[3] Abdullah NAS, Mohamad Z, Khan ZI, Jusoh M, Zakaria ZY, Ngadi N. Alginate based sustainable films and composites for packaging: A review. Chemical Engineering Transactions. 2021;83:271-276.

[4] Rofii MN, Mairing MJ, Listyanto T, Sumardi I, Hartono R. Physical and mechanical properties of laminated board from betung bamboo (Dendrocalamus asper). Journal of the Korean Wood Science and Technology. 2024;52(4):383-392. https://doi.org/10.5658/WOOD.2024.52.4.383

[5] Sulastiningsih IM, Trisatya DR, Indrawan DA, Malik J, Pari R. Physical and mechanical properties of glued laminated bamboo lumber. Journal of Tropical Forest Science. 2021;33(3):290-297. https://doi.org/10.26525/jtfs2021.33.3.290

[6] Sharma B, Gatóo A, Bock M, Ramage M. Engineered bamboo for structural applications. Construction and Building Materials. 2015;81:66-73. https://doi.org/10.1016/j.conbuildmat.2015.01.077
[7] Mahdavi M, Clouston PL, Arwade SR. Development of laminated bamboo lumber: Review of processing, performance, and economical considerations. Journal of Materials in Civil Engineering. 2011;23(7):1036-1042. https://doi.org/10.1061/(ASCE)MT.1943-5533.0000253
[8] Dauletbek A, Li H, Xiong Z, Lorenzo R. A review of mechanical behavior of structural laminated bamboo lumber. Sustainable Structures. 2021;1(1):000004. https://doi.org/10.54113/j.sust.2021.000004
[9] Dauletbek A, Li H, Lorenzo R, Corbi I, Corbi O, Ashraf M. A review of basic mechanical behavior of laminated bamboo lumber. Journal of Renewable Materials. 2022;10(2):273-300. https://doi.org/10.32604/jrm.2022.017805
[10] Sewar Y, Amran M, Avudaiappan S, Gamil Y, Rashid RSM. Bonding strength performance of bamboo-based composite materials: An in-depth insight for sustainable construction applications. Heliyon. 2024;10(13):e32155. https://doi.org/10.1016/j.heliyon.2024.e32155
[11] Darwis Z, Basuki A, Bhayusukma MY, Kristiawan SA, Diharjo K, Wibowo CH, Saputro FN, Majid FM. The mechanical properties of laminated bamboo with different types of adhesive and compression pressures. Engineering, Technology & Applied Science Research. 2026;16(1):31349-31354. https://doi.org/10.48084/etasr.15374
[12] Li H, Wu G, Zhang QS, Deeks AJ, Su J. Ultimate bending capacity evaluation of laminated bamboo lumber beams. Construction and Building Materials. 2018;160:365-375. https://doi.org/10.1016/j.conbuildmat.2017.11.058
[13] Li J, Singh A, Zhou Y. Experimental study on the flexural behavior of I-shaped laminated bamboo composite beam as sustainable structural element. Buildings. 2024;14(3):671. https://doi.org/10.3390/buildings14030671
[14] Khan ZI, Arsad A, Mohamad Z, Habib U, Zaini MAA. Comparative study on the enhancement of thermo-mechanical properties of carbon fiber and glass fiber reinforced epoxy composites. Materials Today: Proceedings. 2021;39:956-958. https://doi.org/10.1016/j.matpr.2020.04.223
[15] Khan ZI, Habib U, Mohamad ZB, Rahmat ARB, Abdullah NASB. Mechanical and thermal properties of sepiolite strengthened thermoplastic polymer nanocomposites: A comprehensive review. Alexandria Engineering Journal. 2022;61(2):975-990. https://doi.org/10.1016/j.aej.2021.06.015
[16] Khan ZI, Mohamad Z, Rahmat AR, Habib U. Synthesis and characterization of composite materials with enhanced thermo-mechanical properties for unmanned aerial vehicles (UAVs) and aerospace technologies. Pertanika Journal of Science and Technology. 2021;29(3):2003-2015. https://doi.org/10.47836/pjst.29.3.15
[17] Li HT, Deeks AJ, Zhang QS, Wu G. Flexural performance of laminated bamboo lumber beams. BioResources. 2016;11(1):929-943. https://doi.org/10.15376/biores.11.1.929-943
[18] Al-Rukaibawi LS, Kachichian M, Károlyi G. Mechanical properties of laminated bamboo lumber N-finity according to ISO 23478-2022. Journal of Wood Science. 2024;70:1. https://doi.org/10.1186/s10086-023-02115-z
[19] Wang X, Zhong Y, Luo X, Ren H. Compressive failure mechanism of structural bamboo scrimber. Polymers. 2021;13(23):4223. https://doi.org/10.3390/polym13234223
[20] Raji AM, Hambali HU, Khan ZI, Mohamad ZB, Azman H, Ogabi R. Emerging trends in flame retardancy of rigid polyurethane foam and its composites: A review. Journal of Cellular Plastics. 2023;59(1):65-122. https://doi.org/10.1177/0021955X221144564